5th International Conference on Biaxial/Multiaxial Fatigue and Fracture
Cracow'97, Poland

J.L. CHABOCHE, J.P. CULIE, F. GALLERNEAU, D. NOUAILHAS,
D. PACOU, D. POIRIER

Thin Wall Thermal Gradient: Experimental Study, F.E. Analysis and Fatigue Life Prediction

Office National d'Etudes et de Recherches Aérospatiales
Direction Scientifique OR
BP 72,
92322 Châtillon Cedex,
FRANCE

Keywords: Thermal gradient - Single crystal superalloy - Finite element analysis - Fatigue life prediction

ABSTRACT: This paper describes a new experimental device designed to produce a thermal gradient in the thickness of thin wall specimens. This device has been applied to polycrystalline and monocrystalline superalloys. Corresponding life predictions, performed by using recent anisotropic models are presented for the single crystal superalloy.

Introduction

Structural components working at high temperature under cyclic conditions are the seat of many complex phenomena. The strong requirements in design procedures (safety, reliability) involve the development of sophisticated lifetime prediction techniques, taking into account the cyclic viscoplastic behaviour as well as crack initiation under creep, oxidation and fatigue conditions. The thermomechanical test is often used to validate constitutive equations and damage models under complex loading situations. Classically, these experiments are performed on thin walled tubes, in order to get an uniform temperature in the thickness of the specimen. This kind of test however may be not

representative enough of the behaviour that can be obtained in components working at high temperature, such as cooled turbine blades, where a very high thermal gradient is generated in a very thin wall.

A specific device has been developed in the laboraty, in order to produce a thermal gradient in the wall of the specimen during a thermomechanical test. This device allows us to generate a gradient of 200°C for an outer temperature of 1050°C, in a tubular specimen of 2 mm thick. Fatigue tests have then been performed under thermomechanical loadings on the monocrystalline superalloy AM1 coated with C_1A chromizing-aluminizing thermal treatment to be as representative as possible of the real blades. The description of the experimental facilities, together with the experimental results, are given in the first section.

A finite element analysis is needed to determine the stress state at the stabilized cycle in each point of the specimen, that must be performed in 3 D in the case of a single-crystal. Prediction for AM1 single crystal requires the use of anisotropic viscoplastic constitutive equations. The results of this analysis are presented in the second section.

The last section gives the application in the most critical areas of the specimen, of a phenomenological fatigue-creep-oxidation interaction model, stress based and recently developed for anisotropic materials, to predict the fatigue life of each test.

Testing equipment and experimental results

In complex highly cooled turbine blades, thermal stresses may become at least as important as the centrifugal stress inducing the creep of the material during the stabilized regime of the engine. Those thermomechanical stresses are particularly produced during take off and landing operations. Thermomechanical fatigue (TMF) tests, in which a volume element is submitted to simultaneous controlled load (or displacement) and temperature, have been developed for turbine blades superalloys over the last 20 years. Those tests provide accurate information on material response but they however do not reproduce the very high thermal gradient due to the cooling of the blade. To simulate the thermal gradient arising to the blade, we have developed a device allowing us to cool the internal wall of a hollow cylindrical fatigue specimen, during the heating of the external wall. The difficulty is to obtain the highest possible thermal gradient but with an acceptable gage section temperature distribution. The heating is obtained with a coil heating fixture connected to a 12-kW audio frequency induction heating unit. One advantage in experiments involving thermal cycling is the time required for heating or cooling which can be kept very short. Another advantage

of using induction unit in this application is the localized nature of the heating of the specimen external surface. The thermal gradient is then produced by cooling the internal surface using a constant pulsed air flow at room temperature as shown on the photo of Fig.1.

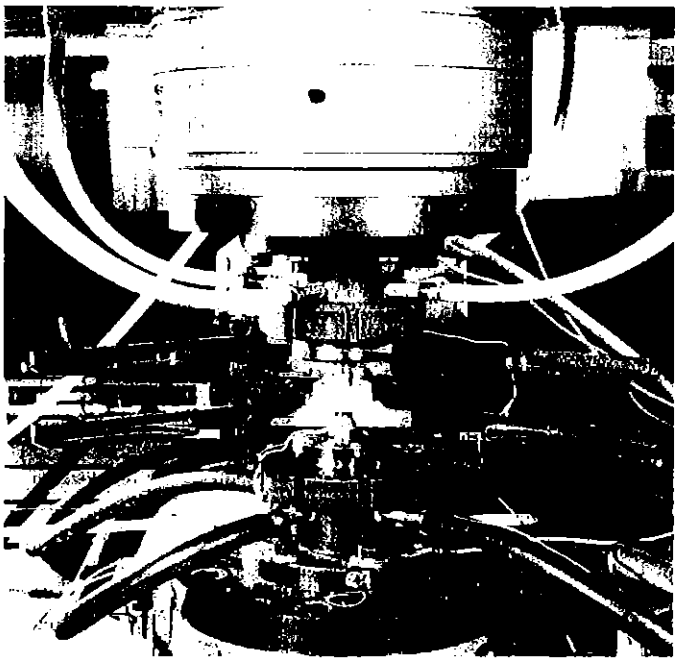

Fig.1 Thin wall thermal gradient experimental device.

A good distribution of the temperature is obtained by means of an alumina sleeve, closed to the internal surface, which induces a cool air flow (Fig.2). A sonic neck system in front of the specimen has been chosen to have a constant and controlled air delivery which can be checked by pressure measurements (by manometers) at the specimen inlet and outlet. Two external temperatures have been studied: 1050°C and 650°C corresponding to the extreme temperatures of the studied TMF cycle. Several thermocouples have been welded on the specimen, on the gage circumference of inner and outer surfaces to verify a good homogeneity of the temperature fields. As it can be seen in the same figure, this experimental facility generates a thermal gradient of 150°C for a maximum external temperature of 650°C and of 200°C for a maximum external temperature of 1050°C, with satisfying temperature fields on the gage circumferences.

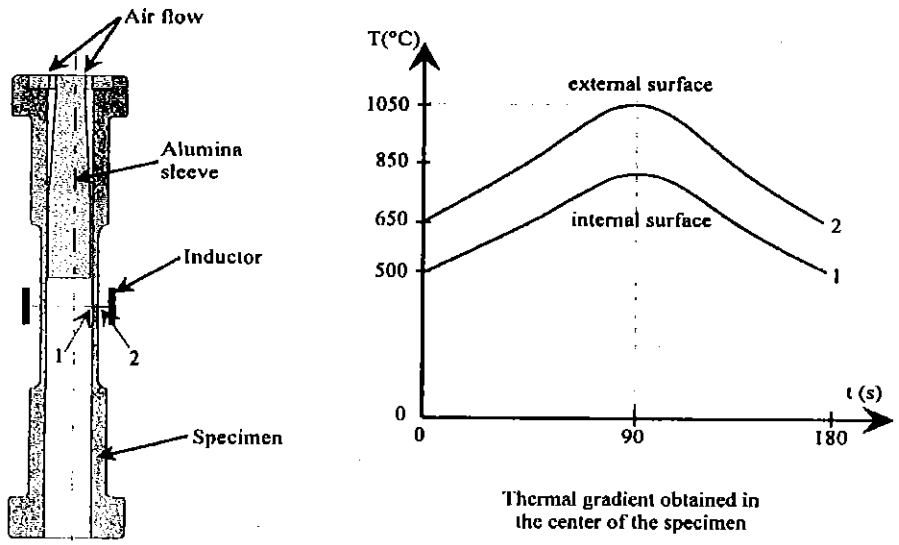

Fig.2 Scheme of the heated/cooled specimen, and temperature distribution.

The TMF cycle used for this study is presented in Fig.3. It consists of a triangular temperature cycle between 650°C and 1050°C, applied on the external wall of the tube, associated with an alternate four slopes stress wave (R_σ=-1). The period of the cycle is 180s.

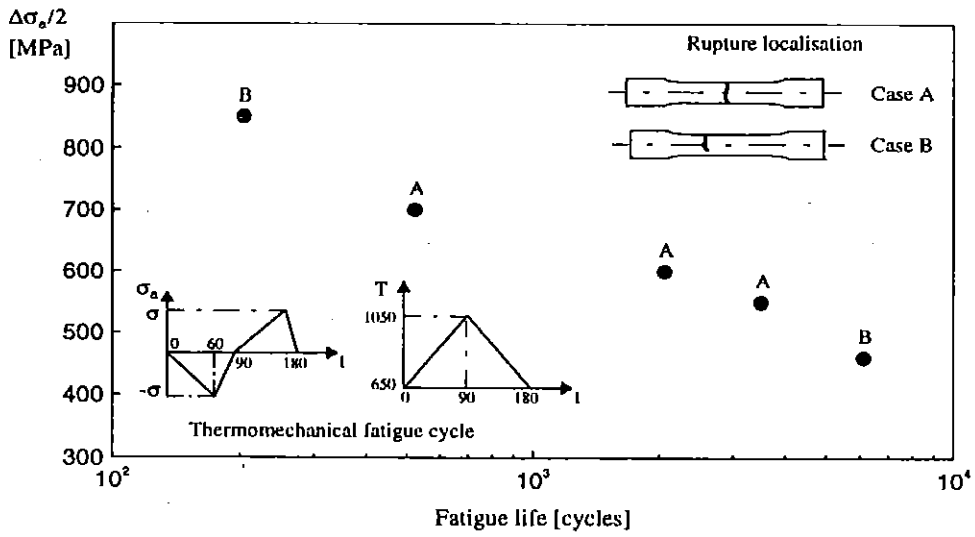

Fig.3 Thermomechanical fatigue cycle and experimental fatigue lifes.

It was defined to simulate the temperature and loading histories at the leading edge region of a turbine blade. Tests are performed on tubular specimens with a wall thickness of 2 mm (external diameter is 14 mm) made of AM1 single crystal superalloy. All the specimens are oriented along the <001> crystallographic orientation. Industrial C_1A coating has been deposited on the external surface of the specimen, as it is made on the real blade, to protect the alloy against oxidation but also against corrosion and erosion phenomena. Experimental lifetimes are plotted in the same figure and we indicated for each test the rupture area.
The observation of rupture zones and breaking surfaces show that two very different rupture mechanisms can happen in spite of a low dispersion of the lifetime. As a matter of fact, the initiation of the macroscopic crack always occurs at the coated external surface but not at the same height z along the specimen generating line. For the lowest and highest stress levels, the rupture occurred in specimen zones where the temperature is low and varies between 200°C and 570°C during the heating cycle. Many cracks have been created at the surface, in the coating, and the observation of the breaking surface reveals that the macroscopic crack is circular. This kind of fatigue damage mechanism has already been observed after isothermal fatigue at a temperature lower than the ductile-brittle temperature of C_1A coating (i.e. around 700°C) (1) (2). For the other tests, the crack initiation occurs in the middle of the specimen where the temperature cycle is the highest (650°C-1050°C). The breaking surface is then very disturbed and is characteristic of an usual fatigue-creep damage mechanism.

Finite element analysis

The determination of the stress-strain state in the specimen requires a finite element analysis. The modelling of single-crystal superalloys behaviour has been widely studied these last years. It has been shown that for these materials, either crystallographic or macroscopic models could predict accurately the cyclic viscoplastic behaviour. Two viscoplastic models are used in this work. The first one is the crystalline model described in (3). This model uses a multicriteria approach, for which the resolved shear stress on each system τ^s is computed from the macroscopic stress tensor and the orientation tensor $\tilde{m}$ of the slip system and one yield criterion is defined for each system. It assumes that the only mechanism of plastic deformation is the crystallographic slip. The viscoplastic strain rate is the result of the contribution of viscoplastic $\dot{\gamma}^s$ shear on the N slip systems. The constitutive

equations are then written on each slip system, with the definition of two scalar variables for each slip system, a kinematic hardening variable and an isotropic one, which is simply the accumulated slip on each system. Cross hardening may be introduced in the expression of the isotropic hardening by means of an interaction matrix. However, no latent hardening has been experimentally observed for the kind of material studied in this work (4) (5), so the interaction matrix reduces to the unity matrix. In fact, the only isotropic hardening is self-hardening, which is present at low temperatures (under 760°C). On the other hand, cube slip is observed even at low temperatures (6). So, two families of material constants are introduced, characterizing the octahedral slip and the cube slip.

The material constants, identified from room temperature to 1100°C on the AM1 alloy were found in (7). As it has been demonstrated in (8), a link can be established between this model and a macroscopic one (9), allowing to deduce the material constants of the macroscopic model from the material constants of the crystallographic one and conversely. Calculations with the macroscopic model are still running, therefore we limit the presentation here to the results obtained with the crystalline model.

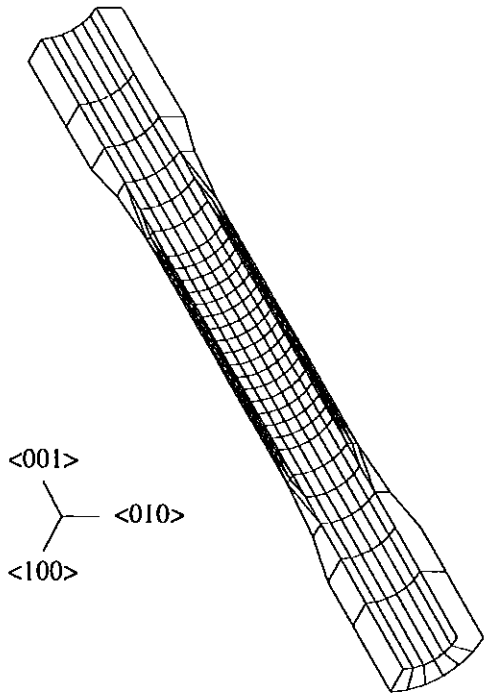

Fig.4 Mesh of the thin wall thermal gradient specimen.

Three dimensions calculations are required for anisotropic material. The mesh of the specimen is shown in Fig.4. Due to the symmetry of the problem, only a quarter of the specimen is computed, for specimen oriented along <001> direction. This mesh is composed of 528 quadratic elements, including four layers of elements in the thickness of the specimen in the central part. Imposed temperatures and loads are shown in the previous section. The five tests have been computed, and we illustrate in fig.5 the axial stress distribution at the maximum of the mechanical loading for an external load of $\sigma = 550$ MPa. It is worth to note that if the stresses are maximum for the maximum temperature (middle of the specimen) at the outer surface (left of fig.5), it is not true for the inner surface (right of fig.5).

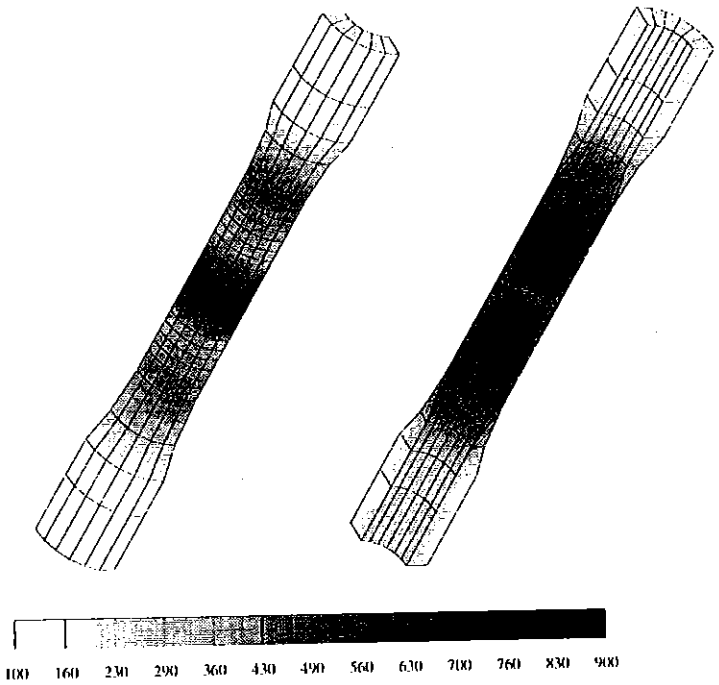

Fig.5 Axial stress contours at the maximum of the mechanical loading, at stabilization.

The next figure (Fig.6) shows the axial (σ_{33}) and circumferential (σ_{22}) stress evolutions, at maximum and minimum of each cycle, and in the centre of the specimen, inside and outside. According to the imposed external load, 30 to 50 cycles were needed to reach the stabilized state. The example is given here for the test at 550 MPa.

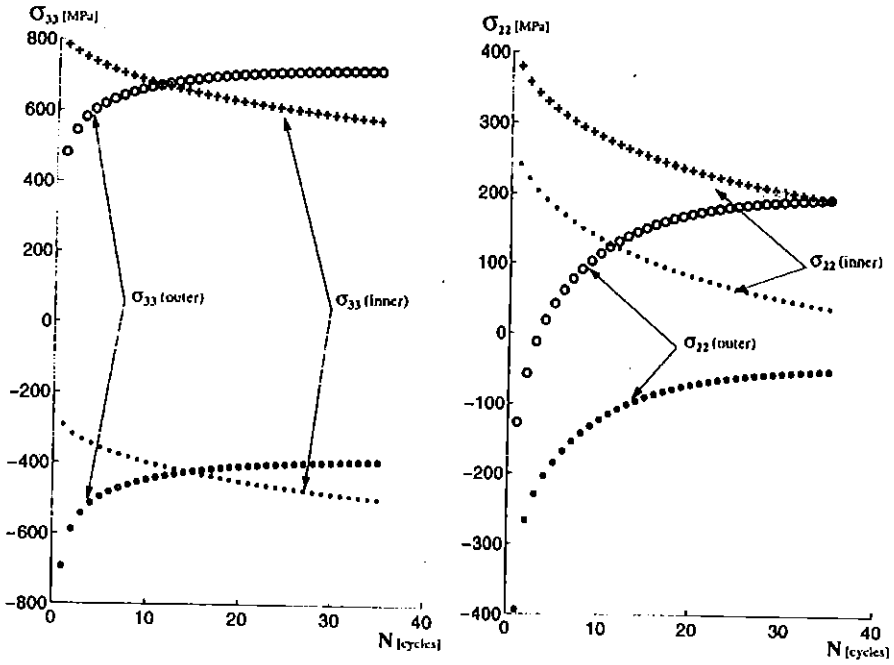

Fig.6 Maximum and minimum stress evolution vs. number of cycles.

Fatigue life prediction

In this section, we present the predictions obtained by the use of a stress based phenomenological fatigue-creep-oxidation interaction model. This model, specifically developed for coated single-crystal superalloys (1) has already been applied successfully to the fatigue life prediction of isothermal and thermomechanical tests but in a configuration of uniaxial stress state.

The model has been detailed elsewhere in its uniaxial (10) and multiaxial (11) forms, and we shortly recall here its main characteristics. To take into account the effect of the coating on the fatigue strength of the superalloy at low temperature, the model differentiates two distinct damage processes: a microinitiation phase and a micropropagation phase respectively described by D_I and D_P variables. Interaction effects are introduced between fatigue and oxidation damage process (traduced by D_{ox} variable) during the microinitiation phase only. The variable D_c is related to creep damage. It can be developed during the microinitiation phase, but it interacts with the fatigue damage during the micropropagation phase.

The important assumption for this model concerns the anisothermal writing (12). As a matter in fact, microinitiation and micropropagation fatigue laws can be suppose temperature independent, by using a notion of reduced stress. These reduced stresses are defined by $S_I = \sigma/\sigma_{uI}(T)$ and $S_P = \sigma/\sigma_{uP}(T)$, and are considered as describing the thermomechanical fatigue cycle, where σ_{uI} and σ_{uP} are respectively the ultimate stresses in microinitiation and in micropropagation which are temperature dependent, the fatigue laws can then be supposed temperature independent. Only time dependent and thermally activated phenomena, such as creep and oxidation, are described by temperature dependent laws.

Damage evolutions due to microinitiation (eqn.(1)) and micropropagation (eqn.(2)) in fatigue, to creep (eqn.(3)) and to oxidation (eqn.(4)) are summarized in Table I. Indices I and P in the equations stand respectively for initiation and propagation. A_{II} is the octahedral shear amplitude, S_{PH} or S_{IH} is the mean hydrostatic pressure as defined by Sines (13), S_{eq} is the Hill equivalent stress. Limit stresses S_i are defined by : $S_{II} = S_{IIo}$ (1-h_1 Mean (tr S_P)), S_{IP} = S_{IPo} (1-h_2 Mean (tr S_P)), and $S_{Iox} = S_{Ioxo}$ (1-h_3 Mean (tr S_P)) + Mean (tr S_P). Similar relation is used for the parameter $M^* = M^*_o$ (1-h_4 Mean (tr S_P)). For damage creep law, Hayhurst's multiaxial criterion (14) has been extended to account for material anisotropy of the single crystal.

This writing makes the model attractive for its identification on a large temperature domain. Pure fatigue tests results performed at one temperature are then sufficient to identify all the parameters of microinitiation and micropropagation laws. Uniaxial isothermal fatigue tests performed at 950°C on AM1 coated C_1A specimens with <001> orientation permit to identify the majority of the parameters (10). Microinitiation and micropropagation laws evolve with temperature through the variations of the ultimate stresses $\sigma_{uI}(T)$ and $\sigma_{uP}(T)$. Fatigue creep tests results conducted at lower frequencies at the same or another temperature allow us to identify the oxidation law. Pure creep tests are nevertheless required to identify the damage creep law at several temperatures. Material anisotropy effects are taken into account by four fourth-order tensor introduced in A_{II} and S_{eq} equations. For cubic anisotropy, only two independent material constants are required. The set of material constants identified over the range of temperature is given in (1).

Table I. Damage growth laws.

$$dD_I = \frac{1}{C}\left\langle \frac{A_{II\,I} - S_{II}(S_{IH})(1-D_{ox})}{(1-D_{ox}) - S_{Ieq\,max}} \right\rangle^{b} dN$$

$$dD_P = \left[1-(1-D_P)^{\beta+1}\right]^{1-a}\left\langle \frac{A_{II\,P} - S_{IP}(S_{PH})}{1-S_{Peqnax}} \right\rangle \left(\frac{A_{IIP}}{M^*(S_{PH})(1-D_P)} \right)^{\beta} dN$$

$$dD_c = \left\langle \frac{\alpha_h \sup_i(\sigma_i) + \beta_h N_c{:}\sigma + (1-\alpha_h-\beta_h)\sqrt{\sigma{:}M_c{:}\sigma}}{A(T)} \right\rangle^{r(T)} (1-D_c)^{-k(T)} dt$$

$$dD_{ox} = \frac{1}{2} D_{ox}^{-1}\left(\frac{K^*}{e_o}\right)\left[1 + \frac{\left\langle \sqrt{S_p^+{:}M_{ox}{:}S_p^+} - S_{lox}\left(S_{PH}\right)\right\rangle}{B}\right]^{2m} dt$$

$$K^{*2} = \frac{1}{\Delta t}\int_o^{\Delta t}\left[K_o \exp\left(-\frac{Q}{RT(t)}\right)\right]^2 dt$$

Predictions made with the data of the stress tensor σ, the time t and the temperature T at the stabilized cycle, for each node located on the outer surface along the generating line of the specimen, in <100> and <110> directions are given in fig.7. In the same figure are plotted the calculated life durations versus the height z along the generating line, for two tests: ($\Delta\sigma/2$ = 700 Mpa ; Nexp = 522) and ($\Delta\sigma/2$ = 460 Mpa ; Nexp = 6126). As it can be seen, only a small difference between the life durations calculated in the two crystallographic orientations is predicted. Anisotropy effects have no important effect on the fatigue life here, due to the fact that the axial stress is dominant. Moreover, for all the studied stress levels, three nodes (marked by the numbers 1, 2 and 3 in Fig.7) along the generating line induce the lowest life durations: one node at the middle of the specimen where the temperature cycle is the highest, and the two others at the both sides of the centre for which the temperature cycle is much lower but where the finite element analysis predicts important stressed zones. The fatigue-creep-oxidation interaction model predicts an important fatigue-

creep-oxidation interaction for the first one at the middle of the specimen. For the others, the life durations are almost consumed by fatigue damage only.

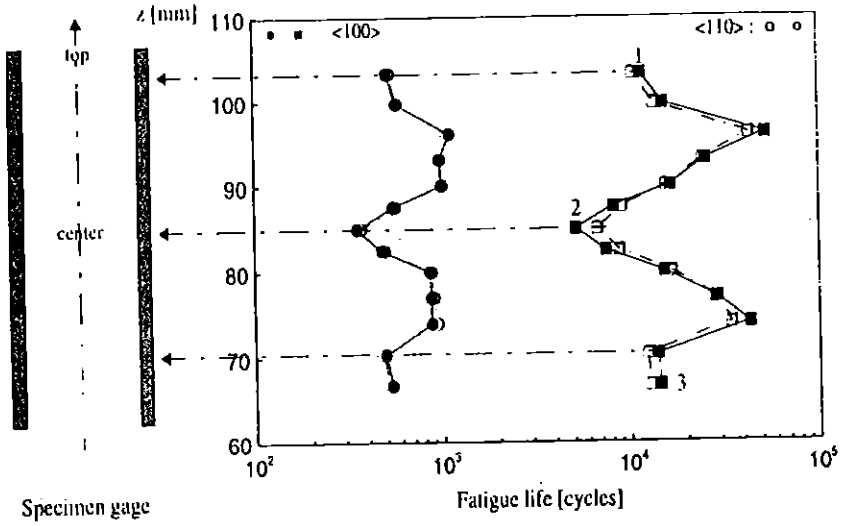

Fig.7 Fatigue life predictions along the specimen gage.

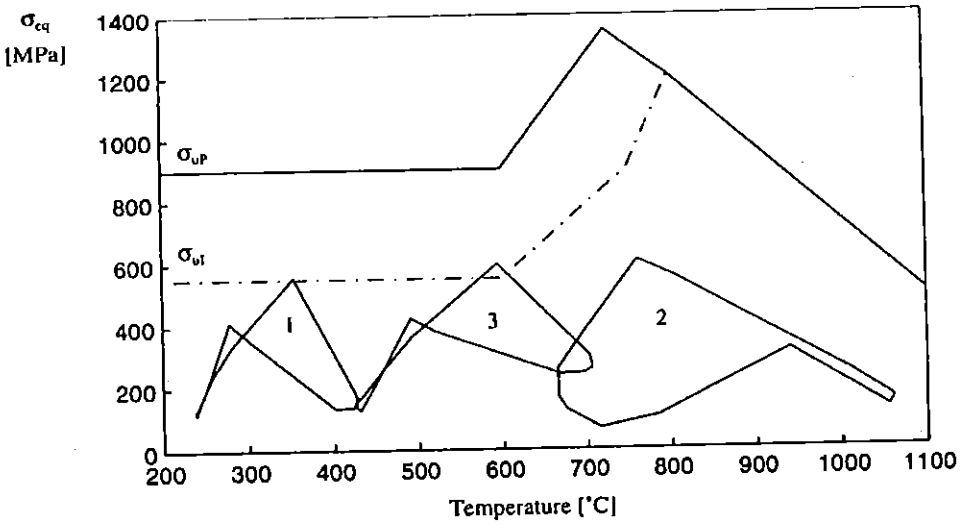

Fig.8 Evolution of the three most damaging stress cycles (equivalent stresses) vs. temperature.

In Fig.8 is given the evolution of the three most damaging stabilized stress cycles with the temperature along the generating line for one test ($\Delta\sigma/2$ = 460 Mpa). In the same figure are plotted the ultimate stresses in initiation and in propagation. At low temperature, below the ductile/brittle transition temperature of C_1A coating, the ultimate stress in initiation (chosen much lower than the propagation one to account for the brittleness of the coating (2) (12)) is raised and it induces a microinitiation period reduced to one cycle in the fatigue damage process. At high temperature, the coating is ductile but oxidation and creep mechanisms, which are thermally activated phenomena, reduce the fatigue life.

The application of the constitutive and damage models allow to find the most damaged zones of the specimen, in agreement with the observation of the breaking surfaces. The small differences between the life durations calculated in those three nodes indicate that the two rupture mechanisms (at low and high temperature) obey to similar damage kinetics. That can explain the fact we observe experimentally the two types of rupture. Finally, the fatigue life of a test is given by the lowest calculated life duration. We have reported in Fig.9 the experimental and predicted lifetimes. A quite good correlation is obtained between the test results and the predictions.

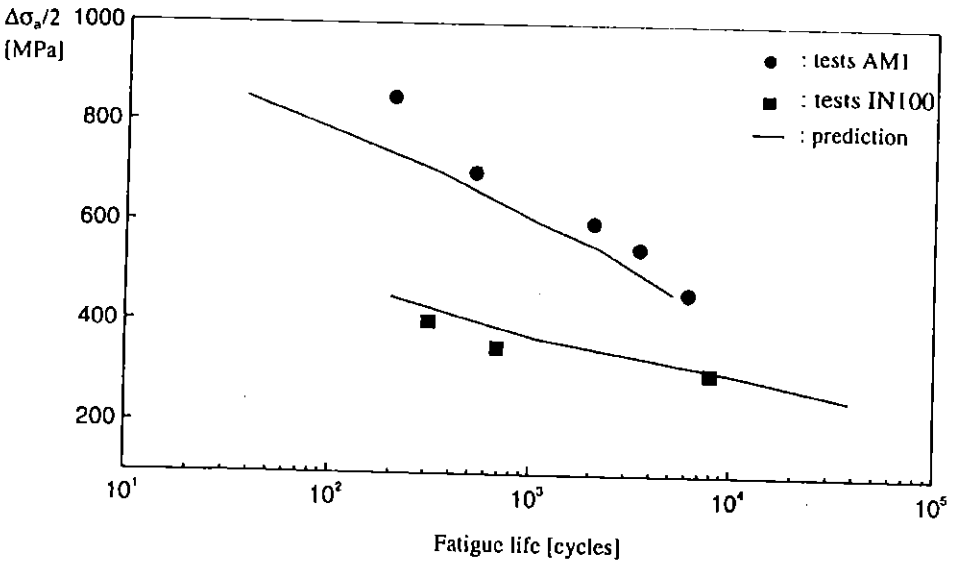

Fig.9 Comparison of experimental and calculated lifetimes.

Results obtained for IN100 polycrystalline superalloy are also plotted in Fig.9 Life predictions performed with former constitutive equations (15) and damage model (16)

developed for isotropic material are also in quite good agreement with the experimental results. It is worth to note also the great benefit in life duration obtained by using single-crystal instead of polycrystalline superalloys.

Conclusion

An experimental device has been developed in order to reproduce in laboratory important thermal gradients in thin walled specimens. That constitutes a very useful tool to test and validate models developed for life prediction of components subjected to complex thermomechanical loading histories. This device has been used on IN100 and AM1 superalloy specimens. Application to the single-crystal superalloy AM1 has been mainly discussed in the paper, as it involves the use of models recently developed.
Life predictions of the set of tests have been performed systematically. A finite element analysis of the specimen is made first by using anisotropic viscoplastic constitutive equations. Then, a fatigue-creep-oxidation interaction damage model is applied as post-treatment of the finite element calculation. The good correlation between tests results and predictions allow to conclude to the ability of these models to be predictive under complex thermomechanical loadings.

References

(1) GALLERNEAU F., (1995), Etude et modélisation de l'endommagement d'un superalliage monocristallin revêtu pour aube de turbine, Thesis, School of Mines of Paris.
(2) CHATAIGNER E. and REMY L., (1995), Influence d'un revêtement protecteur (C_1A) sur la tenue en fatigue d'aubes de turbine monocristallines, Journées de Printemps, Fatigue et traitement de surface, Paris.
(3) MERIC L., POUBANNE P. and CAILLETAUD G., (1991), Single crystal modeling for structural calculations: Part I - Model presentation, Journal of Engn. Mat. and Techn., 113, 162.
(4) WALKER K.P. and JORDAN E.H., (1989), Biaxial constitutive modelling and testing of a single crystal superalloy at elevated temperature, in: Biaxial and multiaxial Fatigue EGF3, Brown M.W., Miller K.J., eds., Mechanical Engineering Publications, London, 145.
(5) MILLIGAN W.W. and ANTOLOVITCH S., (1989), Deformation modeling and constitutive modeling for anisotropic superalloys, NASA Contractor Report 4215.

(6) NOUAILHAS D., PACOU D., CAILLETAUD G., HANRIOT F. and REMY L., (1993), Experimental study of the anisotropic behavior of the CMSX2 single crystal superalloy under tension-torsion loadings, in: Advances in Multiaxial Fatigue, ASTM STP 1191, Mc Dowell D.L., Ellis R., eds., American Society for Testing and Materials, Philadelphia.

(7) De BUSSAC A. and POUBANNE P., (1992), Loi de comportement anisotrope de l'AM1 de 20 à 1100°C, Snecma Technical report YKOM1/YLEV n° 60291.

(8) NOUAILHAS D., CULIE J.P., CAILLETAUD G. and MERIC L., (1995), Finite element analysis of the stress-strain behavior of single-crystal tubes, Eur. J. Mech., A/Solids, 14, n° 1, 137-154.

(9) NOUAILHAS D. and CAILLETAUD G., (1992), Comparaison de divers critères anisotropes pour monocristaux cubiques à face centrée (CFC), Note aux Comptes rendus de l'Académie des Sciences de Paris, t. 315, série II, 1573.

(10) GALLERNEAU F., NOUAILHAS D. and CHABOCHE J.L., (1995), Etude et modélisation de l'endommagement en fatigue d'un superalliage monocristallin revêtu, Journées de Printemps, Fatigue et traitement de surface, Paris.

(11) GALLERNEAU F., NOUAILHAS D.and CHABOCHE J.-L., 1996, A fatigue damage model including interaction effects with oxidation and creep damages, FATIGUE'96, Berlin.

(12) GALLERNEAU F., NOUAILHAS D. and CHABOCHE J.-L., 1996, Fatigue damage behaviour of a coated single crystal superalloy, ESIS'96, Poitiers.

(13) SINES G., (1959), Behavior of metals under complex static and alternating stresses, Metal. Fatigue, 145-169.

(14) HAYHURST D.R., (1972), Creep rupture under multiaxial state of stress, J. Mech. Solids, vol. 20 n° 6, 381-390.

(15) CHABOCHE J.L., (1977), Viscoplastic constitutive equations for the description of cyclic and anisotropic behavior of metals, Bull. de l'Acad. Polonaise des Sciences, série Sc. et Techn., vol. 25, n° 1, 33-42.

(16) LESNE P.M., (1985), Amorçage et propagation de fissures sous gradients thermiques cycliques, thesis,.Publication ONERA 1985 - 2.

Acknowledgements :

Authors would like to gratefully acknowledge Snecma for financial support for the experimental part of this study.